International Journal of Advanced Research in Engineering Innovation
e-ISSN: 2682-8499 | Vol. 2, No. 4, 45-59, 2020
http://myjms.mohe.gov.my/index.php/ijarei

Robeson's Upperbound-Oriented Enhancement of Performance of Hollow Fiber Carbon Membrane for H2/N2 Ideal Separation

Jaya, M. A. T.[1], Jalani, M.A.[1], Yusop, M. F. M.[2], Gonawan, F. N.[2], Nizam, M.K.[3], Ismail, A. F.[4], Ahmad, M. A.[2]

[1] Kolej Permata Insan, Universiti Sains Islam Malaysia, Malaysia
[2] School of Chemical Engineering, Universiti Sains Malaysia, Malaysia
[3] Bio-Aromatics Research Centre of Excellence, Universiti Malaysia Pahang
[4] Advanced Membrane Technology Research Centre, Universiti Teknologi Malaysia, Malaysia

*Corresponding Author: mazani@usim.edu.my, mazani@usim.edu.my, mfirdausyusop@yahoo.com, chfadzil@usm.my, khairulnizam@ump.edu.my, afauzi@utm.my, chazmier@usm.my

Accepted: 1 January 2021 | Published: 15 January 2021

Abstract: *Poly (2,6-dimethyl-1,4-phenylene oxide) (PPO) was successfully converted into hollow fiber carbon membrane for H2/N2 separation study. The ideal separation parameters were enhanced by tuning the pyrolysis temperature, heating rate, and thermal soak time utilizing the Robeson's 2008 upperbound and commercial boundary to obtain maximum balanced point between permeability and ideal selectivity. Using this approach, the optimum H2 permeability and H2/N2 ideal selectivity were 2868 Barrer and 586, respectively. SEM images depicted the surface of the PPO and carbon membrane were both dense, non-porous, symmetrical, and homogeneous. The estimated thickness of the carbon membrane was 14-15 µm. The permeability study indicated that the transport mechanism of the H2 across the membrane layer was dominated by molecular sieving. Excessively high or very low pyrolysis temperature reduced the H2 permeability and H2/N2 ideal selectivity. The H2/N2 ideal selectivity decreased against increasing heating rate as the H2 and N2 permeabilities increased significantly. Thermal soak time was highly effective in increasing the H2 permeability and H2/N2 ideal selectivity. Both H2 permeability and H2/N2 permselectivity from binary test was significantly lower than the ideal separation values due to competitive gas transport through the membrane pore which was completely dominated by the larger N2.*

Keywords: H2/N2 separation, poly (2,6-dimethyl-1,4-phenylene oxide), poly (p-phenylene oxide), optimization, carbon membrane

1. Introduction

Owing to low capital cost and high efficiency in energy consumption, membrane technology in gas separation has been considered as a competitive alternative to replace or integrate with the existing conventional technology such as pressure swing adsorption, cryogenic distillation, and amine absorption [1]. Inorganic membranes, such as carbon membrane, which have good thermal and chemical resistances compared to polymeric membranes, have attracted increasing interest for gas separation under extreme conditions. Such robust membranes are highly promising in natural gas processing, landfill gas recovery, hydrogen recovery, olefin/paraffin separation, and air separation [2– 5].

In early development, most of carbon membranes showed attractive high selectivity but normally at the expense of very low permeability [1]. After years of development, carbon

membrane has shown significant progress towards a more balanced performance, exhibiting both high selectivity and permeability. The capability for separation behavior, known as molecular sieving, is attributed to the pore size approaching the size of diffusing molecules and high porosity, thereby providing massive channels for the diffusion. This turbostratic structure of carbon membrane is able to discriminate gases with similar kinetic diameter, such as O2 and N2.

The development of carbon membrane encompasses several critical variables, such as polymer precursor selection, pyrolysis temperature, heating rate, thermal soaking time, and heating atmosphere. Other variables include polymer structure modification, secondary material, polymer solution concentration, and permeation conditions. In general, the common polymer precursors used for fabricating carbon membrane can be divided into polyimides and non-polyimides. Examples of polyimides are Kapton [6-7], 6FDA-based polyimide [8-10], polyimide BPDA-pp'ODA [11], polyimide BPDA/pPDA [12], polyimide BPDA-DDBT/DABA [13], and Matrimid [14]. Considering the high cost of most of the polyimides, other alternative precursors and non-polyimide polymers have been used, such as poly(vinylidene chloride) [15], poly(furfuryl alcohol) [16,17], phenolic resin [18,19], poly(p-phenylene oxide) [20], and novolac resin [21].

Recently, hydrogen recovery has been receiving researchers' attention because of the increasing demand of hydrogen, which is widely utilized in petroleum industry, particularly hydroalkylation, hydroesulfurization, and hydrocracking. Hydrogen is also regarded as an environmentally friendly energy carrier [22]. The hydrogen production requires separation and purification from other byproducts, such as N2 in ammonia production. The research progress on carbon membrane for H2/N2 separation is summarized in Figure 1, which presents several excellent carbon membranes. The highest H2 permeability was 6080 Barrer [23], 5387 Barrer [24], and 5100 Barrer [25], which were produced using unsupported thin films of phenol-formaldehyde (PFR) and resorcinol-formaldehyde (RFR) resins as precursors. The highest H2/N2 permselectivity was 1086 [26], 725 [27], and 614.7 [28], which were produced using cellophane paper, tubular supported PFR/alumina, and thin film polypyrrolone, respectively, as precursors. Tanco et al. [27] fabricated an optimum carbon membrane that exhibited the best balance between permeability and permselectivity, which were 1731.3 Barrer and 725, respectively, with respect to the Robeson's 2008 upperbound [46] and commercial boundary [47]. The membrane was produced by vacuum-assisted dip-coating of mixture of PFR and boehmite sol, and then pyrolyzed at 550 °C with heating rate and thermal soaking time of 1 °C/min and 2 h, respectively. The membrane was aged for 24 h and reactivated before testing. The deposited water reacted with the carbon active sites and formed oxygen functional groups, which caused a decrease in pore size that effectively hindered the N2 diffusion.

Improving the performance of carbon membrane is to increase the membrane productivity and efficiency. The selectivity and permeability need to be balanced and they are unique for different gases separation. Extremely high selectivity but extremely low permeability or vice versa is undesirable. Previous works had suggested several ways to improve the performance of carbon membrane by adding secondary materials [41, 44, 45], discovering new materials [36, 34, 25], and altering the microstructure of the polymeric precursor [43, 20]. However, the values of the performance fall outside the desirable region. Therefore, Robeson's upperbound [46] and the suggested boundary of commercially attractive [47] as shown in Figure 1 can be used to guide the researchers to ensure the improvement of the permeability and selectivity is oriented to fall within the boundary and the desirable optimum points can be obtained. From this point, necessary improvement such as addition of secondary materials can be continued

accordingly. It has been reported that the microstructure of carbon membrane, in which eventually determines the gas diffusion and selectivity, can be controlled and adjusted by controlling the pyrolysis parameters which are pyrolysis temperature, heating rate and soak time [48]. This work is to show that the carbon membrane pyrolysis and its corresponding performances can be directed into the optimum area of desirable permeability and selectivity. This is a simple and new approach to enhance the carbon membrane performance without integrating or introducing new secondary materials, or creating new or micro-altering precursors. According to [49], the pyrolysis temperature is the most dominant factor in affecting the permeability and ideal selectivity, followed by heating rate and thermal soak time which is used in this study.

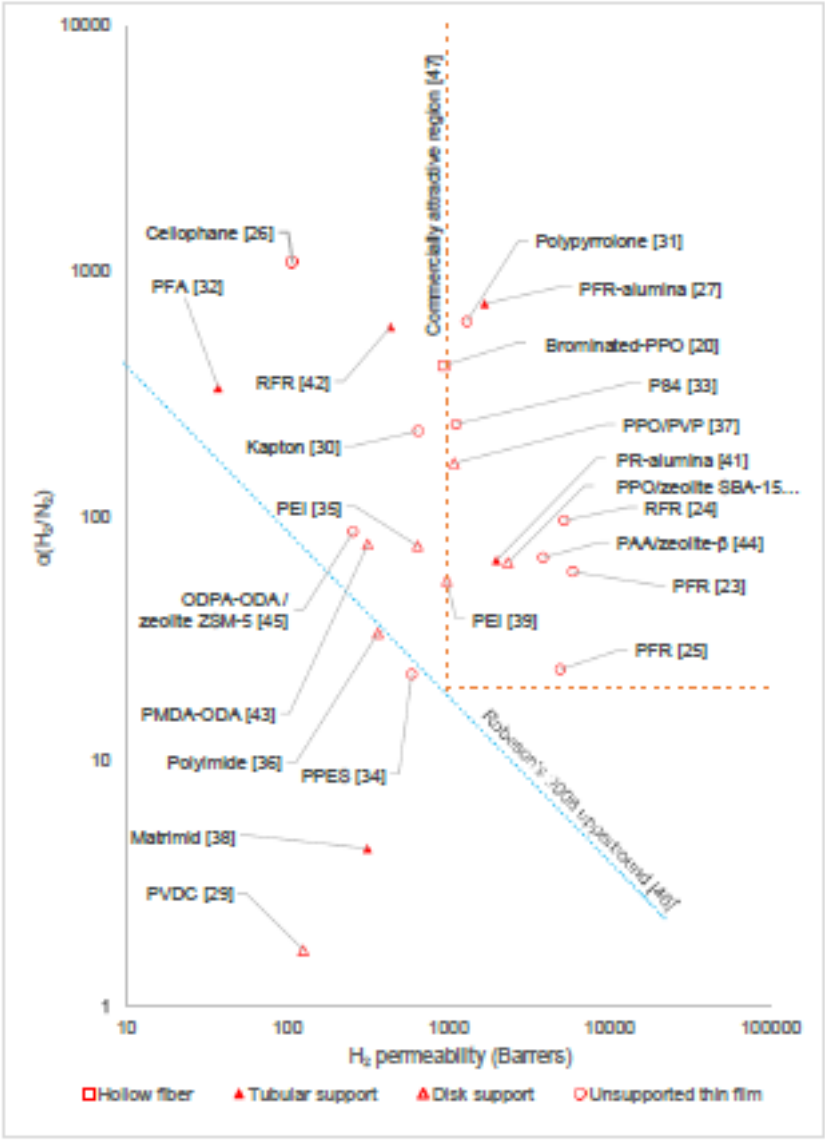

Figure 1: H2/N2 performance of carbon membranes compared with the Robeson's 2008 upperbound

2. Research Methodology

Materials and Method

The PPO powder was purchased from Sigma-Aldrich (US). A 20 wt% of PPO polymer solution was prepared using chloroform (purity 99.5%) as the solvent with vigorous stirring (1000 rpm)

for 30 mins. Before it was spun into hollow fiber polymeric membrane, the polymer solution was left for 30 mins at room temperature. The polymer solution was spun into hollow fiber with the following parameters; air gap: 25cm; polymer solution flowrate: 0.25g/min; bore fluid: 125 ml/hr ethanol; receiving bath: ethanol.

The freshly spun hollow fiber was left inside the bath for a day, cut, and dried in oven for 30 mins. The fiber was thermostabilized at 240 °C for 45 mins under continuous supply of air (50 ml/min) and followed by pyrolysis under continuous nitrogen supply (50 ml/min). The pyrolysis temperature, heating rate, and thermal soak time were varied. All samples were kept inside a tight-closed desiccator.

Scanning electron microscope (SEM, Model Quanta FEG 450, FEI, USA) was used to capture the images of the samples' cross sections to analyse the morphology and estimate their thickness. Since the carbon membrane was brittle, epoxy was used to coat the samples before it was broken. The samples were crushed into powder for X-ray diffraction (XRD, Model PW 1820, Philips, USA) analysis to analyse the crystallinity of the samples. Small fragments of the samples were sent for thermogravimetric (TGA, Model STA6000, Perkin Elmer, USA) analysis.

Constant-pressure/variable-volume system was adopted to estimate the membrane flowrate in which soap-bubble flow meter was used. For single permeability test, the membrane fiber was bore-sided fed in which it was sealed at one end, and opened at the other end to received pressurized gas. The test was began with H2, followed by CH4, and CO2. The H2 was also used to purge the membrane between the transitions from CH4 to CO2. The feed gauge pressure was 3.0 bar. The reading was taken after 18 hours of steady state.

For binary mixture experiment, the membrane was open-ended at both ends. The schematic diagram is showed in Figure 2. The mixing tank was continuously purged to atmosphere at 10ml/min to preserve the feed concentration. The concentration of the feed gas was tuned using flow rate controllers and fine- tuned using pressure regulators placed before the controllers. The retentate was controlled with flow controller.

3. Results and Discussion

Morphology of the PPO and carbon membranes

SEM images of the PPO and carbon membranes' cross-sectional views were depicted in Figures 2 which indicated the membrane structures were non-porous, dense, homogeneous and symmetrical. The estimated thickness of the carbon membrane was 14-15 μm. The change of the morphology is due to thermal rearrangement during the pyrolysis (Xu et al., 2011)[50]. It also involves partial decomposition of the polymer PPO in the thermostabilization stage and pyrolysis (Rivaton, 1995)[51] as well as compaction (Sazali et al., 2015)[52].

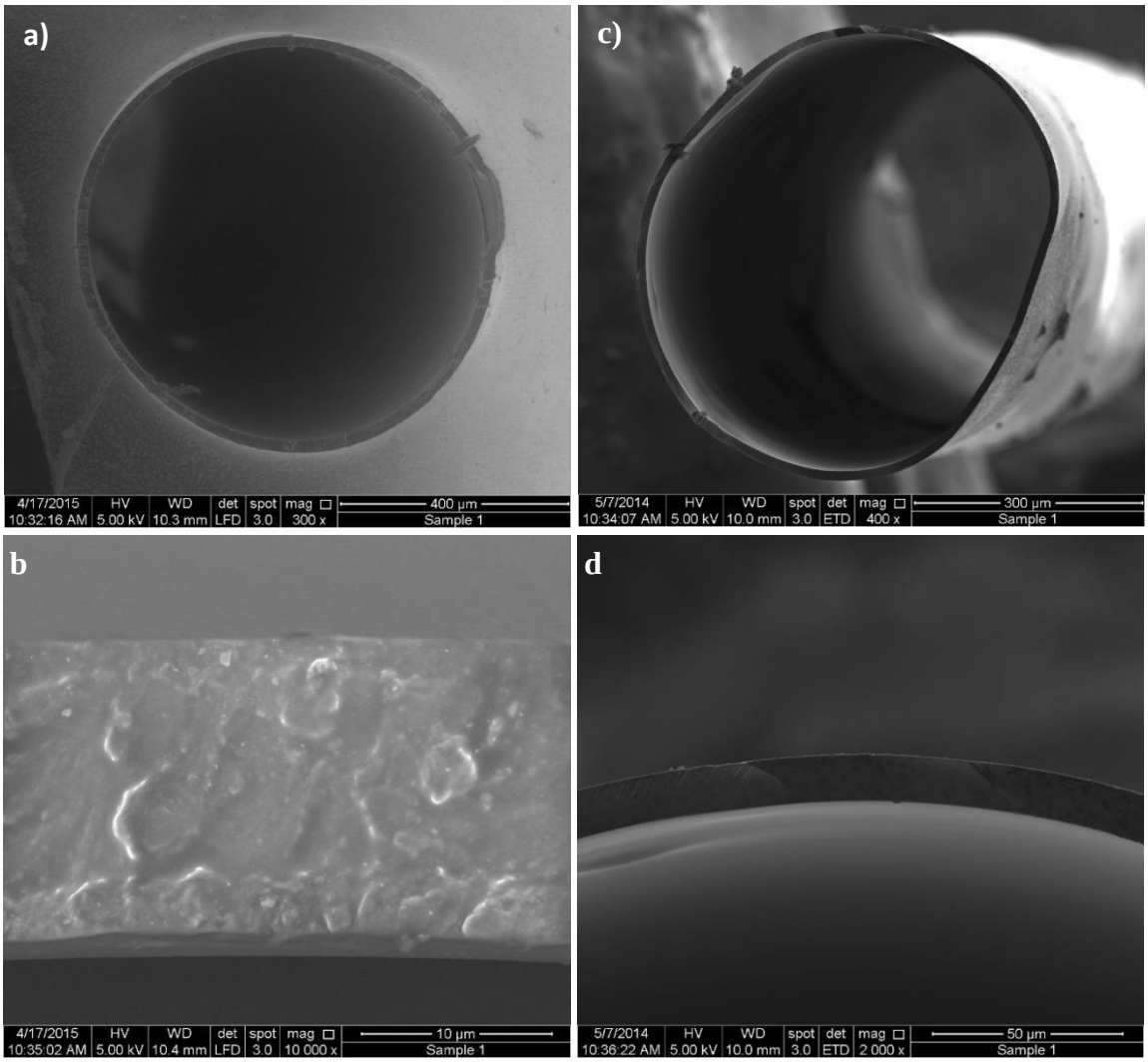

Figure 2: Physical and SEM images of cross-sectional views of PPO membrane (a, b) and carbon membrane (c, d)

Transport mechanism of the carbon membranes

In carbon membrane, there are normally three possibilities of transport of gases molecules through its structure which are Knudsen diffusion, selective surface diffusion and molecular sieving depending mostly on the nature of pore structure and pore size [53]. Figure 3 shows the permeabilities of H2, CO2, O2, CH4 and N2 for the carbon membranes pyrolyzed at 500 °C (CM500), 600 °C (CM600) and 700 °C (CM700) with heating rate and thermal soak time of 1 °C/min and 0.25 hr, respectively. PPOM permeability was included for comparison purpose. The order of the gas on the x-axis was arranged according to the order of the gas kinetic diameters starting from the smallest (H2) to the largest (CH4). The decreasing trend of the permeabilities against the increasing kinetic diameter of the gases, as shown by the PPOM and CM600, suggested that the transport mechanism was governed by molecular sieving effect [49][37][54].

The permeabilities of all gases except CO2 dropped significantly when the sample was pyrolyzed to 500 °C due to the pre-mature development of porous structure. As suggested by the TGA analysis in sub-chapter 4.3.3, at this pyrolysis stage, the decomposition of gases and structure rearrangement to create highly porous structure was not sufficient for the diffusion of most non-adsorbable gases. These decomposed gases were responsible in creating the

microporous channels on their way out [23][55][56]. The amorphous structure originated from the thermostabilized PPOM gradually collapsed during the pyrolysis and chaotically rearranged as amorphous carbon [57].

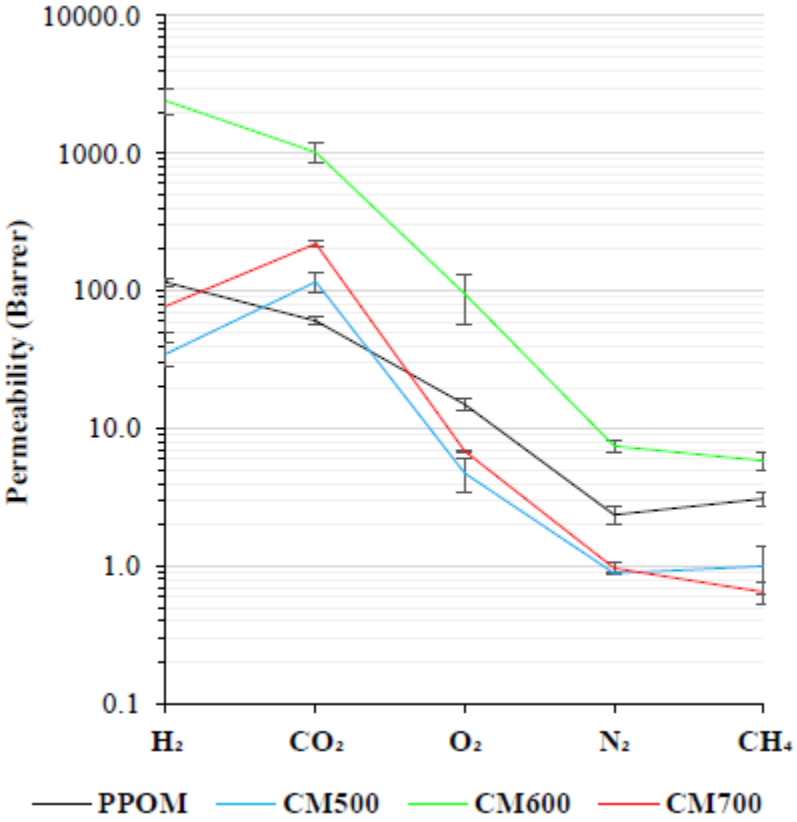

Figure 3: Permeabilities by carbon membrane prepared at different pyrolysis temperatures

H2 permeability and H2/N2 ideal selectivity of carbon membrane against pyrolysis temperature

The permeabilities of H2 and N2, and H2/N2 ideal selectivity against pyrolysis temperature are shown in Figure 4. After the PPO membrane was thermostabilized, and then pyrolyzed at 500 °C, significant reductions of H2 and N2 permeabilities and H2/N2 ideal selectivity were observed because of the pre-mature development of porous structure. During the thermostablization, the PPOM underwent oxidative crosslinking, which caused the formation of highly-packed polymer chains in the membrane structure [51]. The decomposition of gases started to occur during the pyrolysis, which created the micro-channels when the decomposing gases were released [58]. The decomposition occurred simultaneously with thermal shrinkage, which was triggered by the increasing temperature on the membrane structure [52].

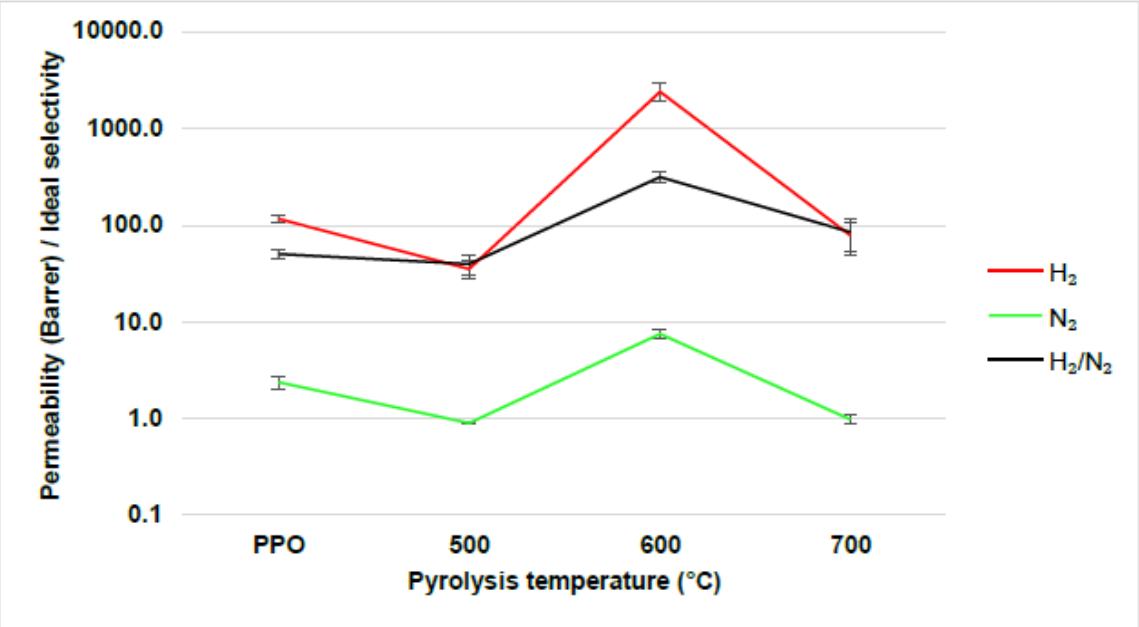

Figure 4: Permeabilities of H2 and N2 and H2/N2 ideal selectivity by PPO membrane and its carbon derivatives

When the pyrolysis temperature was increased from 500 to 600 °C, the H2 and N2 permeabilities increased significantly from 35.2 Barrer to 2401.9 Barrer and from 0.9 Barrer to 7.5 Barrer, respectively. The H2/N2 ideal selectivity was significantly increased as well given that the magnitude of increment of H2 permeability was relatively higher. This phenomenon was an indication of well-developed pore structure with high porosity and ideal pore size for the separation. This phenomenon was believed to be due to the dehydrogenation, in which massive amount of hydrogen gas was released to establish membrane structure with high porosity [59]. The release also purged most of the entrapped and large decomposed gases, such as carbon monoxide and carbon dioxide. The result also showed the absence of trade-off behavior between H2 permeability and H2/N2 ideal selectivity. Similar observation was shown by previous work [26]. As the pyrolysis temperature was increased to 700 °C, the H2 and N2 permeabilities, and H2/N2 ideal selectivity decreased significantly because of thermal shrinkage, which led to decreased pore size and porosity [60]. At this stage, the thermal shrinkage was more dominant than gaseous decomposition factor. Based on the Robeson's 2008 upperbound in Figure 5a, CM600 was the optimum carbon membrane for further enhancement.

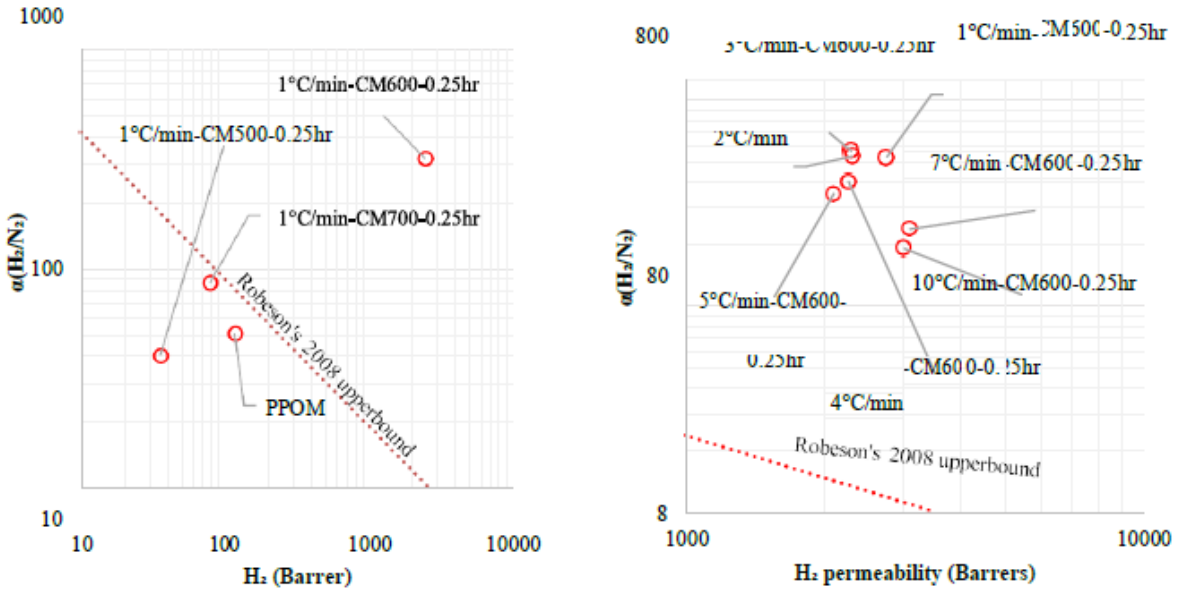

a) pyrolysis temperature b) heating rate

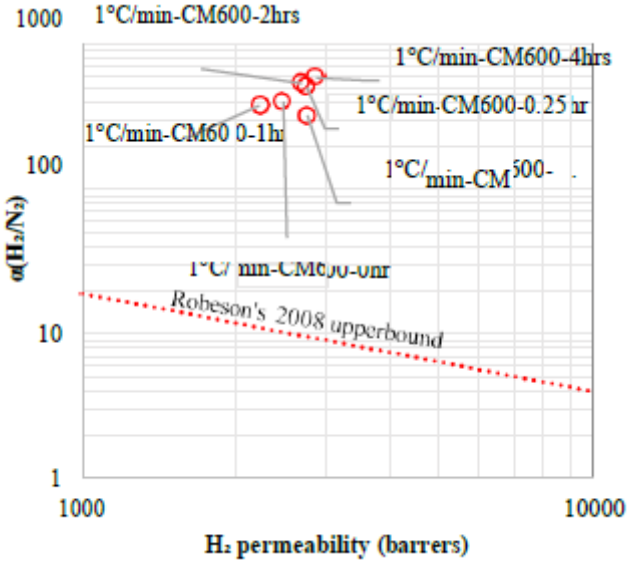

c) thermal soak time

Figure 5: Performances of the PPO and carbon membranes against Robeson's 2008 H2/N2 upperbound at different pyrolysis conditions

H2 permeability and H2/N2 ideal selectivity of carbon membrane against heating rate

The heating rate was varied in the pyrolysis of CM600 with thermal soaking time of 0.25 h, as shown in Figure 6. The H2 permeability indicated a slight increase after heating rate at 7 and 10 °C/min. The increment of N2 permeability can be clearly seen from the decrease of H2/N2 ideal selectivity starting at 4 °C/min. The increase of permeabilities with increasing heating rate indicated that the CM600 received minimum impact of thermal shrinkage because of shorter period of thermal exposure. In addition, the endothermic decomposition would also cause cooling effect that minimized the shrinkage effect on the pore structure. The lack of thermal shrinkage effect left the pore developed by the decomposing gases large in size, which had caused a significant reduction in the H2/N2 ideal selectivity. The thermal shrinkage during the pyrolysis was highly effective at slower heating rate region (1–3 °C/min). The effect can

be seen from the high H2/N2 ideal selectivity with only a slight decrease of H2 permeability as compared with that at higher heating rates. According to Robeson's 2008 upperbound in Figure 5b, 1 °C/min was the optimum heating rate to obtain CM600 with the best H2/N2 separation performance.

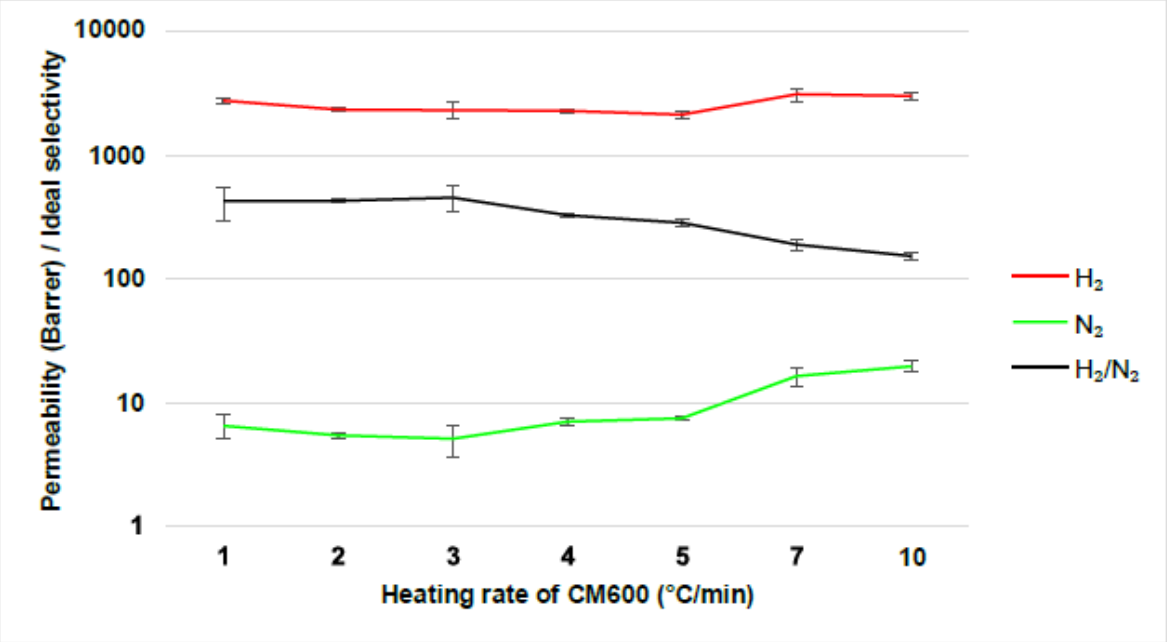

Figure 6: Permeabilities of H2 and N2, and H2/N2 ideal selectivity of CM600 against pyrolysis heating rate

H2 permeability and H2/N2 ideal selectivity of carbon membrane against thermal soaking time

Figure 7 shows the H2/N2 permeability plot of sample 1 °C/min-CM600 against thermal soaking time. The H2 and N2 permeabilities indicated consistent increase when thermal soak time was applied from 0 to 0.5 h. The H2 and N2 permeabilities increased from 2474 and 6.2 to 2756 and 8.7 Barrer, respectively. The pore structure of the carbon membrane continued to develop as the decomposition continued. Besides that, some of the pores developed earlier was cleansed from entrapped decomposing gases.

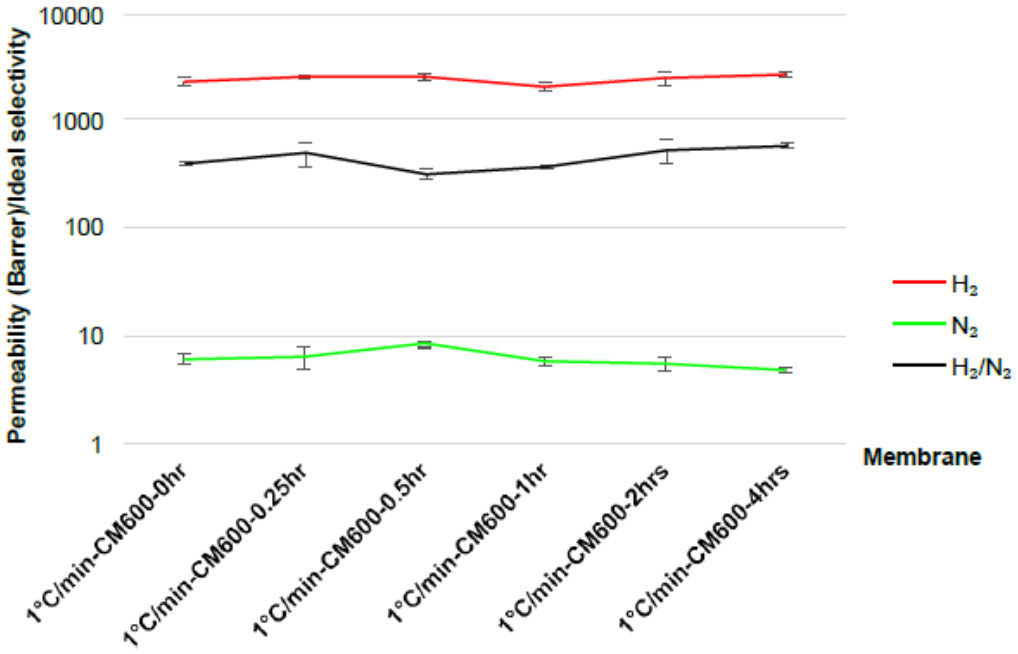

Figure 7: H2 and N2 permeabilities and H2/N2 ideal selectivities of 4 °C/min-CM600 against thermal soaking time

However, further increase of thermal soak time to 4 h caused the N2 permeability to gradually decrease, while the H2 permeability remained consistent. This was a clear indication of thermal sintering effect which reduced the membrane pore size and densified the pore structure [56]. The effect was more dominant against the larger N2 than the H2 indicating the porosity remained high since the decomposition replaced some of the pore collapsed due to the sintering effect [60]. The increase of N2 permeability against thermal soaking time of 0 to 0.5 h decreased the H2/N2 ideal selectivity. On the other hand, the consistency of H2 permeability and gradual decrease of N2 permeability against the thermal soaking time between 1 to 4 h resulted in a significant increase of H2/N2 ideal selectivity from 322 to 586. This result indicated that the membrane pores can be fine-tuned at micro-scale by utilizing the thermal soak time, to create pore structure that obstruct large gases, with minimum impact on the smaller ones. As a result, the ideal selectivity of the H2/N2 was found to be at maximum at longer thermal soaking time. According to the Robeson's 2008 upperbound in Figure 5c, the best thermal soaking time for optimum H2/N2 separation performance was 4 h. The carbon membrane samples became highly fragile and brittle after 8 h of thermal soaking which shattered after exposure to gas pressure higher than 1 bar. As shown in Figure 8, some samples were tore open because of extreme densification; the tear was as wide as 0.25 mm.

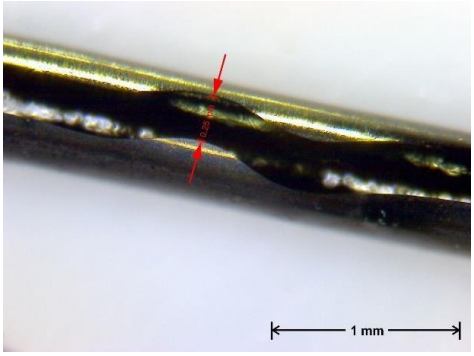

Figure 8: Physical appearance of 1 °C/min-CM600 after 8 h of thermal soaking showing a tear stretching along the fiber

Figure 9 shows the CM600s after enhancement. The results are plotted together with that from previous works against Robeson's 2008 upperbound. The figures provide an overview of the current membranes in comparison with that in previous works for future improvement. Based on the single gas test, the performance of 1 °C/min-CM600-4 h hollow fiber carbon molecular sieve membrane was competitive. In addition, a balance between H2/N2 ideal selectivity and H2 permeability was observed compared with the PFR-based tubular supported carbon membrane by [27]. However, the 1 °C/min- CM600-4 h was located under Robeson's 2008 upperbound for the mixture test because of extremely low H2/N2 permselectivity.

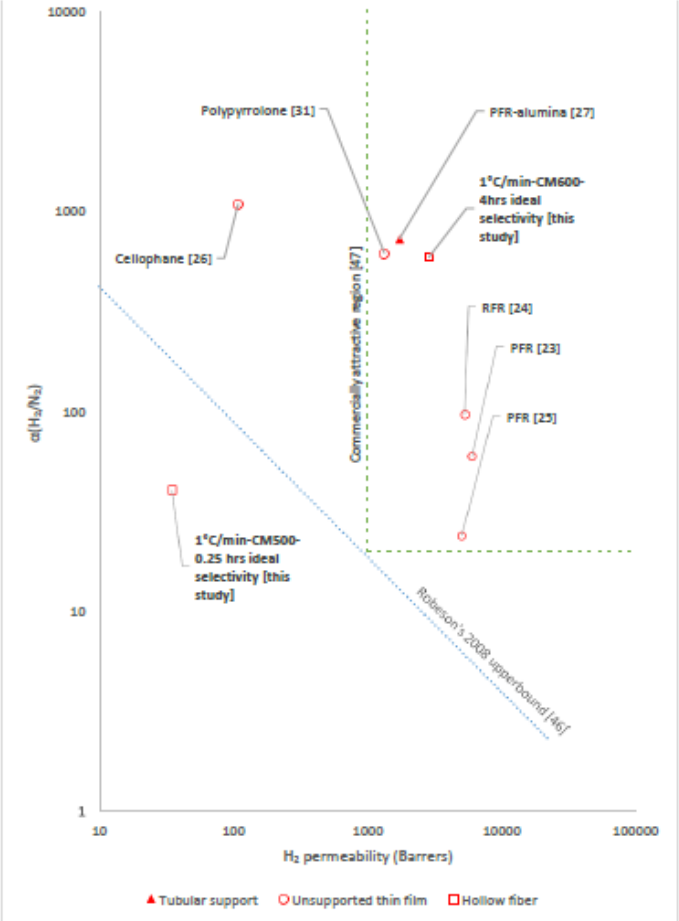

Figure 9: Performance of optimized CM600 in the current work and carbon membranes from previous works against Robeson's 2008 H2/N2 upperbound

4. Conclusion

This paper presented the synthesis and enhancement of hollow fiber carbon membrane from PPO in terms of pyrolysis temperature, heating rate, and thermal soaking time based on the Robeson's upperbound and H2/N2 commercial boundary. The surface morphology of the 14-15-µm-thick carbon membrane was dense, homogeneous and symmetrical. The structure of the carbon membrane was amorphous, and the transport mechanism of H2 through the carbon membrane was dominated by molecular sieving. High pyrolysis temperature reduced the H2 permeability and H2/N2 ideal selectivity. Increasing the heating rate increased the H2 and N2 permeabilities but decreased the H2/N2 ideal selectivity. Increasing the thermal soaking time slightly increased the H2 permeability and decreased the N2 permeability, which resulted in increased H2/N2 ideal selectivity. The well-balanced H2 permeability and H2/N2 ideal selectivity from the single gas test were 2868.2 Barrer and 586, respectively. The study has

shown that the carbon membrane performance enhancement through pyrolysis parameter adjustment, control which can be well integrated to ensure the permeability and ideal selectivity obtained is within the desirable region.

References

1. Ismail, A., & David, L. (2001). A review on the latest development of carbon membranes for gas separation. Journal of Membrane Science, 193, 1-18.
2. Koros, W. J. & Mahajan R. (2000). Pushing the limits on possibilities for large scale gas separation: which strategies? Journal of Membrane Science, 175, 181-196.
3. White, L. S., Blinka, T. A., Kloczewski, H. A. & Wang, I. (1995). Properties of a polyimide gas separation membrane in nautral gas streams. Journal of Membrane Science, 103, 73-82.
4. Bhide, B. D. & Stern, S. A. (1993). Membrane processes for the removal of acid gases from natural gas. I. Process configuration and optimization of operating conditions, Journal of Membrane Science, 81, 209-237.
5. Kim Y. K., Park, H. B. & Lee, Y. M. (2003). Carbon molecular sieve membrane derived from metal-substituted sulfonated polyimide and their gas separation properties, Journal of Membrane Science, 226,145-158.
6. Hatori, H., Yamada, Y., & Shiraishi, M. (1992). Preparation of macroporous carbon films from polyimide by phase-inversion method. Carbon, 30(2), 303-304.
7. Suda, H., & Haraya, K. (1995). Molecular sieving effect of carbonized Kapton polyimide membrane. Journal of the Chemical Society, Chemical Communications, 1179-1180.
8. Jones, C., & Koros, W. (1994). Carbon molecular sieve gas separation membranes-I. Preparation and characterization based on polyimide precursors. Carbon, 32(8), 1419-1425.
9. Geiszler, V., & Koros, W. (1996). Effects of polyimide pyrolysis conditions on carbon molecular sieve membrane properties. Industrial and Engineering Chemistry Research, 35, 2999-3003.
10. Ma, X., Lin, Y., Wei, X., & Kniep, J. (2016). Ultrathin carbon molecular sieve membrane for propylene/propane separation. AlChE Journal, 62(2), 491-499.
11. Hayashi, J., Mizuta, H., Yamamoto, M., Kusakabe, K., & Morooka, S. (1997). Pore size control of carbonized BPDA-pp'ODA polyimide membrane by chemical vapor deposition of carbon. Journal of Membrane Science, 124, 243-251.
12. Fuertes, A., & Centeno, T. (1998). Preparation of supported asymmetric carbon molecular sieve membranes. Journal of Membrane Science, 144, 105-111.
13. Okamoto, K., Kawamura, S., Yoshino, M., Kita, H., Hirayama, Y., Tanihara, N., & Kusuki, Y. (1999). Olefin/paraffin separation through carbonized membranes derived from an asymmetric polyimide hollow fiber membrane. Industrial and Engineering Chemistry Research, 38, 4424- 4432.
14. Sazali, N., Salleh, W., Nordin, N., Harun, Z., & Ismail, A. (2015). Matrimid-based carbon tubular membranes: The effect of the polymer composition. Journal of Applied Polymer Science.
15. Rao, M., & Sircar, S. (1993). Nanoporous carbon membranes for separation of gas mixtures by selective surface flow. Journal of Membrane Science, 85, 253-264.
16. Chen, Y., & Yang, R. (1994). Preparation of carbon molecular sieve membrane and diffusion of binary mixtures in the membrane. Industrial and Engineering Chemistry Research, 33, 3146- 3153.

17. Acharya, M., Raich, B., Foley, H., Harold, M., & Lerou, J. (1997). Metal-supported carbogenic molecular sieve membranes: Synthesis and Applications. Industrial and Engineering Chemistry Research, 36, 2924-2930.
18. Katsaros, F., Steriotis, T., Stubos, A., Mitropoulos, A., Kanellopoulos, N., & Tennison, S. (1997). High pressure gas permeability of microporous carbon membranes. Microporous Materials, 8, 171-176.
19. Centeno, T., & Fuertes, A. (1999). Supported carbon molecular sieve membranes based on a phenolic resin. Journal of Membrane Science, 160, 201-211.
20. Yoshimune, M., Fujiwara, I., Suda, H., & Haraya, K. (2005). Novel Carbon Molecular Sieve Membranes Derived from Poly(phenylene oxide) and Its Derivatives for Gas Separation. Chemistry Letters, 34(7), 958-959.
21. Tanco, M., Tanaka, D., Rodrigues, S., Texeira, M., & Mendes, A. (2015). Composite-alumina- carbon molecular sieve membranes prepared from novolac resin and boehmite. Part I: Preparation, characterization and gas permeation studies. International Journal of Hydrogen Energy, 40, 5653-5663.
22. Yun, S. & Oyama, T. (2011). Correlations in palladium membranes for hydrogen separation: A review, Journal of Membrane Science, 375, 28-45.
23. Wang, S., Zeng, M., & Wang, Z. (1996). Carbon membranes for gas separation. Separation Science and Technology, 31(16), 2299-2306.
24. Zhang, B., Dang, X., Wu, Y., & Liu, H. (2014). Structure and gas permeation of nanoporous carbon membranes based on RF resin/F-127 with variable catalysts. J. Mater. Res., 29(23), 2881- 2890.
25. Shusen, W., Meiyun, Z., & Zhizhong, W. (1996). Asymmetric molecular sieve carbon membranes. Journal of Membrane Science, 109, 267-270.
26. Campo, M., Magalhaes, F., & Mendes, A. (2010). Carbon molecular sieve membranes from cellophane paper. Journal of Membrane Science, 350, 180-188.
27. Tanco, M., Tanaka, D., & Mendes, A. (2015). Composite-alumina-carbon molecular sieve membranes prepared from novolac resin and boehmite. Part II: Effect of the carbonization temperature on the gas permeation properties. International Journal of Hydrogen Energy, 40, 3485-3496.
28. Kita, H., Yoshiko, M., Tanaka, K., & Okamoto, K. (1997). Gas permselectivity of carbonized polypyrrolone membrane. Chemical Communication, 1051-1052.
29. Rao, M., & Sircar, S. (1993). Nanoporous carbon membranes for separation of gas mixtures by selective surface flow. Journal of Membrane Science, 85, 253-264.
30. Suda, H., & Haraya, K. (1997). Gas permeation through micropores of carbon molecular sieve membranes derived from Kapton polyimide. The Journal of Physical Chemistry B, 101, 3988- 3994.
31. Kita, H., Yoshiko, M., Tanaka, K., & Okamoto, K. (1997). Gas permselectivity of carbonized polypyrrolone membrane. Chemical Communication, 1051-1052.
32. Shiflett, M., & Foley, H. (1999). Ultrasonic deposition of high-selectivity nanoporous carbon membranes. Science, 285, 1902-1905.
33. Hosseini, S., & Chung, T. (2009). Carbon membranes from blends of PBI and polyimides for N2/CH4 and CO2/CH4 separation and hydrogen purification. Journal of Membrane Science, 328, 174-185.
34. Zhang, B., Shen, G., Wu, Y., Wang, T., Qiu, J., Xu, T., & Fu, C. (2009). Preparation and characterization of carbon membranes derived from poly(phthalazinone ether sulfone) for gas separation. Industrial and Engineering Chemistry Research, 2886-2890, 48.
35. Tseng, H., Shiu, P., & Lin, Y. (2011). Effect of mesoporous silica modification on the structure of hybrid carbon membrane for hydrogen separation. Internation Journal of Hydrogen Energy, 36, 15352-15363.

36. Itta, A., & Tseng, H. (2011). Hydrogen separation performance of CMS membranes derived from the imide-functional group of two similar types of precursors. International Journal of Hydrogen Energy, 36, 8645-8657.
37. Itta, A., Tseng, H., & Wey, M. (2011). Fabrication and characterization of PPO/PVP blend carbon molecular sieve membranes for H2/N2 and H2/CH4 separation. Journal of Membrane Science, 372, 387-395.
38. Briceno, K., Montane, D., Garcia-Valls, R., Iulianelli, A., & Basile, A. (2012). Fabrication variables affecting the structure and properties of supported carbon molecular sieve membranes for hydrogen separation. Journal of Membrane Science, 415-416, 288-297.
39. Tseng, H., Shih, K., Shiu, P., & Wey, M. (2012). Influence of support structure on the permeation behavior of polyetherimide-derived carbon molecular sieve composite membrane. Journal of Membrane Science, 405-406, 250-260.
40. Tseng, H., Itta, A., Weng, T., & Li, Y. (2013). SBA-15/CMS composite membrane for H2 purification and CO2 capture: Effect of pore size, pore volume, and loading weight on separation performance. Microporous and Mesoporous Materials, 180, 270-279.
41. Teixeira, M., Rodrigues, S., Campo, M., Tanaka, D., Tanco, M., Madeira, L., . . . Mendes, A. (2014). Boehmite-phenolic resincarbonmolecularsieve membranes—Permeationandadsorptionstudies. Chemical Engineering Research and Design, 92, 2668-2680.
42. Rodrigues, S., Whitley, R., & Mendes, A. (2014). Preparation and characterization of carbon molecular sieve membranes based on resorcinol-formaldehyde resin. Journal of Membrane Science, 459, 207-216.
43. Li, L., Song, C., Jiang, H., Qiu, J., & Wang, T. (2014). Preparation and gas separation performance of supported carbon membranes with ordered mesoporous carbon interlayer. Journal of Membrane Science, 450, 469-477.
44. Li, L., Wang, C., Wang, N., Cao, Y., & Wang, T. (2015). The preparation and gas separation properties of zeolite/carbon hybrid membranes. Journal of Materials Science, 50, 2561-2570.
45. Zhang, B., Wu, Y., Lu, Y., Wang, T., Jian, X., & Qiu, J. (2015). Preparation and characterization of carbon and carbon/zeolite membranes from ODPA-ODA type polyetherimide. Journal of Membrane Science, 474, 114-121.
46. Robeson, L. (2008). The upper bound revisited. Journal of Membrane Science, 320, 390-400.
47. Go, Y., Lee, J. H., Shamsudin, I. K., Kim, J., & Othman, M. R. (2016). Microporous ZIF-7 membranes prepared by in-situ growth method for hydrogen separation. International Journal of Hydrogen Energy, 41(24), 10366-10373.
48. Saufi, S. M., & Ismail, A. F. (2004). Fabrication of carbon membranes for gas separation––a review. Carbon, 42(2), 241-259.
49. He, X., & Hagg, M. B. (2011). Optimization of carbonization process for preparation of high performance hollow fiber carbon membranes. Industrial & Engineering Chemistry Research, 50(13), 8065-8072.
50. Xu, L., Rungta, M., & Koros, W. J. (2011). Matrimid® derived carbon molecular sieve hollow fiber membranes for ethylene/ethane separation. Journal of membrane science, 380(1-2), 138- 147.
51. Rivaton, A. (1995). Photochemical and thermal oxidation of poly (2, 6-dimethyl-1, 4-phenylene oxide). Polymer degradation and stability, 49(1), 11-20.
52. Sazali, N., Salleh, W. N. W., Md Nordin, N. A. H., Harun, Z., & Ismail, A. F. (2015). Matrimid- based carbon tubular membranes: The effect of the polymer composition. Journal of Applied Polymer Science, 132(33).

53. Li, L., Wang, T., Liu, Q., Cao, Y., & Qiu, J. (2012). A high CO2 permselective mesoporous silica/carbon composite membrane for CO2 separation. Carbon, 50(14), 5186-5195.
54. Zhang, B., Wang, T., Zhang, S., Qiu, J., & Jian, X. (2006). Preparation and characterization of carbon membranes made from poly (phthalazinone ether sulfone ketone). Carbon, 44(13), 2764- 2769.
55. Wei, W., Qin, G., Hu, H., You, L., & Chen, G. (2007). Preparation of supported carbon molecular sieve membrane from novolac phenol–formaldehyde resin. Journal of Membrane Science, 303(1-2), 80-85.
56. Salleh, W. N. W., & Ismail, A. F. (2012). Fabrication and characterization of PEI/PVP-based carbon hollow fiber membranes for CO2/CH4 and CO2/N2 separation. AIChE Journal, 58(10), 3167-3175.
57. Lua, A. C., & Su, J. (2006). Effects of carbonisation on pore evolution and gas permeation properties of carbon membranes from Kapton® polyimide. Carbon, 44(14), 2964-2972.
58. Fu, S., Sanders, E. S., Kulkarni, S. S., & Koros, W. J. (2015). Carbon molecular sieve membrane structure–property relationships for four novel 6FDA based polyimide precursors. Journal of Membrane Science, 487, 60-73.
59. Foley, H. C. (1995). Carbogenic molecular sieves: synthesis, properties and applications. Microporous Materials, 4(6), 407-433.
60. Salleh, W. N. W., Ismail, A. F., Matsuura, T., & Abdullah, M. S. (2011). Precursor selection and process conditions in the preparation of carbon membrane for gas separation: A review. Separation & Purification Reviews, 40(4), 261-311.